Active site dynamics in the zinc-dependent medium chain alcohol dehydrogenase superfamily

Patrick J. Baker[a,1], K. Linda Britton[a], Martin Fisher[a], Julia Esclapez[b], Carmen Pire[b], Maria Jose Bonete[b], Juan Ferrer[b], and David W. Rice[a]

[a]The Krebs Institute, Department of Molecular Biology and Biotechnology, University of Sheffield, Western Bank, Sheffield S10 2TN, United Kingdom; and [b]Departamento de Agroquimica y Bioquimica, Division de Bioquimica y Biologia Molecular, Facultad Ciencias, Universidad Alicante, Ap99, E-03080 Alicante, Spain

Edited by Stephen J. Benkovic, Pennsylvania State University, University Park, PA, and approved November 21, 2008 (received for review August 1, 2008)

Despite being the subject of intensive investigations, many aspects of the mechanism of the zinc-dependent medium chain alcohol dehydrogenase (MDR) superfamily remain contentious. We have determined the high-resolution structures of a series of binary and ternary complexes of glucose dehydrogenase, an MDR enzyme from *Haloferax mediterranei*. In stark contrast to the textbook MDR mechanism in which the zinc ion is proposed to remain stationary and attached to a common set of protein ligands, analysis of these structures reveals that in each complex, there are dramatic differences in the nature of the zinc ligation. These changes arise as a direct consequence of linked movements of the zinc ion, a zinc-bound bound water molecule, and the substrate during progression through the reaction. These results provide evidence for the molecular basis of proton traffic during catalysis, a structural explanation for pentacoordinate zinc ion intermediates, a unifying view for the observed patterns of metal ligation in the MDR family, and highlight the importance of dynamic fluctuations at the metal center in changing the electrostatic potential in the active site, thereby influencing the proton traffic and hydride transfer events.

MDR family | structure | zinc metalloenzyme | reaction mechanism

Zinc-dependent enzymes catalyze many important cellular processes (1); yet, despite this, the role played by the zinc ion in catalysis is not completely understood, partly because zinc is silent in a range of useful spectroscopic techniques, such as EPR and optical spectroscopy. One of the best characterized zinc-containing enzyme families is the Zn-dependent medium chain alcohol dehydrogenase superfamily (MDR), which catalyzes the oxidation of primary or secondary alcohols to the corresponding aldehydes or ketones using $NAD(P)^+$ as a cofactor (2).

The structures of many MDR family members have been determined with that of liver alcohol dehydrogenase (LADH) as the prototypical member (3). These studies have shown that the subunit of these enzymes is constructed from two domains, a nucleotide binding domain and a catalytic domain (4), with the essential zinc ion located deep in the cleft between them. The ligands to the zinc are provided by residues from the catalytic domain and, in the absence of substrate, the zinc is coordinated to the side chains of three well conserved residues, which in LADH are Cys-46, His-67, and Cys-174 (2). The tetrahedral coordination shell of the zinc is completed by a water molecule (2).

In the classical text book mechanism for this enzyme family (5), this zinc-bound water molecule is suggested to be displaced by the incoming hydroxyl group of the alcohol on substrate binding, to leave the zinc ion coordinated to the substrate and the same three protein ligands as in the apo enzyme. The redox reaction requires the net removal of two hydrogen atoms from the substrate and is thought to proceed via proton loss from the substrate hydroxyl to bulk solvent by using a proton relay system to form an alkoxide intermediate that is stabilized by the positive charge on the enzyme-bound zinc ion. Subsequent collapse of the intermediate to the ketone with concomitant hydride transfer to $NAD(P)^+$ completes the reaction. In this mechanism, the zinc ion is believed to be tetrahedrally coordinated to the same protein ligands throughout the enzyme's catalytic cycle.

In an alternative view of catalysis by this enzyme family, a different reaction mechanism has been suggested, based in part on EPR measurements of Co^{2+}-substituted LADH in which the zinc-bound water molecule remains coordinated to the metal, serving as a site for transient proton transfer and predicting the formation of penta-coordinated zinc intermediates (6–9). Recent time-resolved X-ray absorption fine structure analysis (XAFS) on the alcohol dehydrogenase from *Thermoanaerobacter brockii* (10) has provided supporting evidence for this alternative mechanism by identifying a series of intermediates that includes a water molecule in the zinc-coordination sphere and differs both in the coordination number of the zinc ion and the zinc-ligand bond distances. These results have been interpreted as suggesting that two distinct five coordinated zinc species are present during the reaction cycle. The possibility of penta-coordinated zinc intermediates is further supported by the structure of the MDR enzyme human sorbitol dehydrogenase in complex with NADH, Zn^{2+}, and an hydroxymethylated pyrimidine-based inhibitor that shows that the zinc is coordinated by two protein ligands, a water molecule and two atoms from the inhibitor (11).

Further uncertainties in the mechanism concern the role of a highly conserved acidic residue in the enzyme family (Glu-68 in LADH), which lies close to, but not coordinating, the zinc in the active site. This residue has been suggested to be involved in catalysis, either as a structural residue to stabilize the geometry of the active site (12), as a moderator of the electrostatic potential near the substrate (13), or, alternatively, as a possible zinc ligand during the enzyme's catalytic cycle (14–16). A recent atomic resolution structure of LADH in complex with NADH and Zn provides some evidence for different positions of the zinc-bound water and alternative conformations for Glu-68, indicating its potential as a zinc ligand (17).

Glucose dehydrogenase (GlcDH) from the extremely halophilic archaeon *Haloferax mediterranei* is an MDR enzyme, which catalyzes the first step of a modified version of the

Author contributions: P.J.B., M.J.B., and D.W.R. designed research; P.J.B., K.L.B., M.F., J.E., C.P., and J.F. performed research; J.E., C.P., M.J.B., and J.F. contributed new reagents/analytic tools; P.J.B., K.L.B., J.E., M.J.B., and D.W.R. analyzed data; and P.J.B. and D.W.R. wrote the paper.

The authors declare no conflict of interest.

This article is a PNAS Direct Submission.

Data deposition: The coordinates and structure factors of the GlcDH complexes have been deposited in the Protein Data Bank, www.pdb.org (PDB ID codes: 2vwp, 2vwq, 2vwh, and 2vwg).

[1]To whom correspondence should be addressed. Email: P.Baker@sheffield.ac.uk.

This article contains supporting information online at www.pnas.org/cgi/content/full/0807529106/DCSupplemental.

Entner-Doudoroff pathway of glucose catabolism, interconverting ß-D-glucose to gluconolactone, with $NADP^+$ as the preferred coenzyme. The mechanism is sequential with D-glucose binding after $NADP^+$, followed by the ordered release of gluconolactone and NADPH (18). The protein is a homo-dimer with a subunit molecular weight of 39 kDa (357 residues) and requires zinc for catalysis (18–20). The structures of the apo enzyme and a D38C mutant in complex with $NADP^+$ and zinc have been determined (21) and reveal that the subunit, like that of the other MDR family members, is organized into two domains separated by a deep cleft, with the active site lying at its base. Domain 1 (residues 1–168 and 301–357) contains the residues involved in substrate binding, catalysis, and coordinating the active site zinc, with domain 2 (residues 169–300) consisting of a dinucleotide-binding Rossmann fold (22) that is responsible for binding $NADP^+$.

To contribute to a deeper understanding of the mechanism in the MDR family, we have determined a series of X-ray crystal structures of ligand complexes of *H. mediterranei* GlcDH. To our knowledge, these are the widest range of high-resolution binary and ternary complexes seen for any MDR family enzyme. Analysis of these structures shows that although the conformation of the residues in the active site of the various complexes are closely related, the zinc ligands interchange during catalysis as a result of coordinated movements of both the zinc and its bound water within the active site.

Results and Discussion

The structures of *H.mediterranei* GlcDH in binary complexes with either $NADP^+/Zn^{2+}$ or $NADPH/Zn^{2+}$, a ternary complex with $NADP^+/Zn^{2+}$ /glucose, and a nonproductive ternary complex with $NADP^+/Zn^{2+}$ /gluconolactone were determined from isomorphous crystals to 2.0-Å resolution. In these crystals, the asymmetric unit contains one subunit of the biologically active dimer.

In each complex clear electron density could be assigned in the active site for the dinucleotide, the enzyme-bound zinc ion, and either a ring closed glucose or gluconolactone, as appropriate. An additional electron-density feature, assigned to a water molecule (W1), could be seen to coordinate the zinc in each complex. The NADP(H) binds at the C-terminal end of the beta sheet facing the cleft between the two domains, with the nicotinamide moiety lying at the base of the cleft adjacent to the essential zinc. In the ternary complexes, either the lactone or glucose are in the chair conformation, with C1 approximately 3.4 Å from C4 of the nicotinamide ring and in an ideal orientation for hydride transfer. All of the ring hydroxyls form hydrogen bonds to the protein: the side chains of Glu-114 and His-49 to O6; Glu-114 to O4; Asn-303 to O3; and Glu-150 to O2.

Loop Closure on Substrate Binding. Superposition of the structures of the $NADPH/Zn^{2+}$ binary complex with the $NADP^+/Zn^{2+}$/glucose or $NADP^+/Zn^{2+}$/lactone ternary complexes shows that the binding of glucose or lactone to the enzyme triggers a large conformational change to the loop (residues 47–53) joining helix α1 and strand βe, which closes in on the active site, reducing the solvent accessibility. As a consequence, the side chain of His-49, which in the $NADPH/Zn^{2+}$ complex points out toward the solvent, moves some 15 Å to hydrogen bond to the O6 hydroxyl of the glucose or lactone substrate (see supporting information (SI) Fig. S1). This movement is linked, in turn, to a translation of helix α1 (residues 39–46) some 1.8 Å toward the active site, with concomitant changes to the side chain torsion angles of Asp-38, which then becomes a ligand to the zinc ion. Torsion angle changes to the side chain of Thr-40 result in its side chain oxygen lying within hydrogen bonding distance of the C1 hydroxyl of the substrate and the 2′ hydroxyl of the nicotinamide ribose. Thus the concerted movement on substrate binding of the 47–53 loop and α1 can be thought of as a coupled lever and a piston, whose motion has the dual effect of promoting substrate binding and reorganising the ligands to the catalytic zinc.

Dynamic Changes at the Zinc Center during Catalysis. With the exception of the conformational change affecting the position of α1 and, in particular, Asp-38, superposition of the active sites of the four complexes reveals that the residues in the vicinity of the catalytic zinc adopt almost identical positions (Fig. 1). In contrast, detailed comparisons show that there are significant changes in the position of the zinc ion and its associated water molecule, W1, within the static cage provided by the active site, which result in distinct patterns of ligation of the zinc and the water by the protein in the different complexes. The side chains of four residues (Asp-38, His-63, Glu-64, and Glu-150), the water molecule (W1), and the substrate C1 oxygen lie in the vicinity of the zinc and provide six possible ligands. In the structures of each of the complexes, the zinc is tetrahedrally coordinated, but three different patterns of ligation from protein residues to the zinc ion are observed, with only one protein ligand, His-63, being constant between them (Table 1).

In the two binary complexes with either the oxidized or reduced cofactor, the zinc forms ligands to three protein side chains (His-63, Glu-64, and Glu-150) and the water molecule, W1 (Fig. 1*A*). A superimposition of the structures of the $NADPH/Zn^{2+}$ binary and the $NADP^+/Zn^{2+}$ /glucose ternary complexes, shows that the atoms belonging to His-63, Glu-64, and Glu-150 overlap closely (0.25-Å rmsd over 28 atoms). However, in the transition between these two complexes, the zinc moves some 1.4 Å away from the side chains of Glu-150 and Glu-64, and W1 moves 1.2 Å in the opposite direction, to mediate their interaction with the zinc. Thus, in the ternary complex with glucose, Asp-38 and O1 of the glucose replace Glu-150 and Glu-64 as zinc ligands, with W1 remaining coordinated to the zinc, but from a different relative position to that seen in the binary complex (Fig. 1*B*).

Comparing the ternary complex with glucose to that with lactone, the zinc ligands undergo more changes as a result of further movements of the zinc ion and W1, with each moving by approximately 1.0 Å, again in opposite directions. Between these two ternary complexes the atoms of residues Asp-38, His-63, Glu-64, and Glu-150 remain in essentially identical positions (0.15-Å rmsd over 36 atoms), with the zinc ion moving away from O1 of the glucose and toward OE2 of Glu-64, to leave the substrate hydroxyl outside the zinc coordination sphere, and replaced by Glu-64 as a zinc ligand (Fig. 1*D*). The zinc-bound water, W1, moves away from Glu-64, to lie within hydrogen bonding distance of the substrate C2 hydroxyl and mediating the interaction of Glu-150 with the zinc ion (Fig. 1*C*).

The crystallographic studies presented here identify quite different patterns of zinc ligation in the active sites of the binary and two ternary complexes. Whilst a water molecule remains coordinated to the zinc ion in each complex, its position in the coordination sphere is from a different vertex in the tetrahedral arrangement of the ligands around the zinc (Fig. 2, Fig. S2, and Movie S1). Although we cannot be certain that the movements seen here are in not some way constrained by the crystal lattice, the fact that the loop carrying His-49 moves by up to 15 Å, with the associated movement of helix α1, upon soaking the $NADP^+$/Zn/GlcDH crystals with either glucose or lactone, shows that the crystals can accommodate large scale movements at the active site, consistent with the crystal packing contacts occurring at the periphery of the subunits, far removed from the active site cleft.

Comparison to MDR Family Members. Despite the widespread attention that has been paid to members of the MDR superfamily, there remain relatively few examples of high-resolution substrate complexes with the wild-type enzyme, except for those

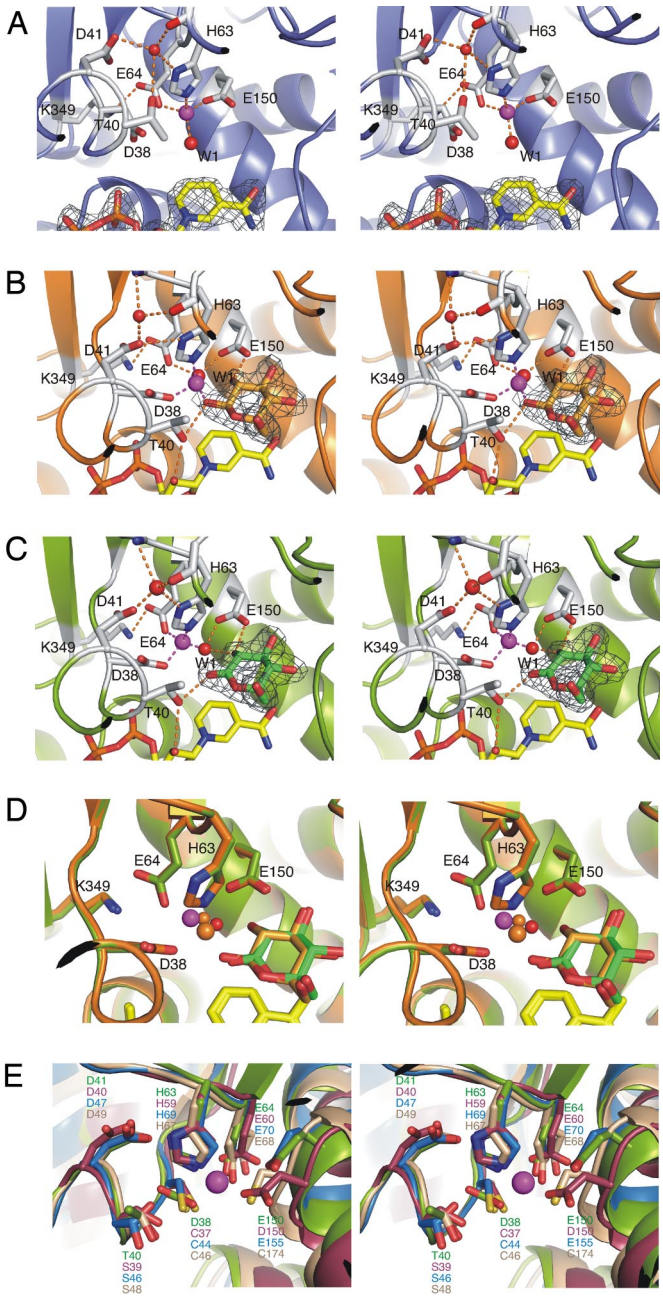

Fig. 1. The active site of the glucose dehydrogenase binary and ternary complexes. (*A–E*) The protein is shown as a cartoon, with residues highlighted in the text in atom representation. The NADP(H) is shown as sticks (yellow carbons) with the catalytic zinc (magenta) and 2 water molecules (red) shown as spheres. The sigmaA mF_O-DF_C electron density map for the various substrates, contoured at 1σ, is shown as gray lines. (*A*) The NADPH/Zn structure (blue carbons), (*B*) the $NADP^+$/Zn/glucose structure (orange carbons), (*C*) the $NADP^+$/Zn/gluconolactone structure (green carbons), (*D*) an overlap of the $NADP^+$/Zn/gluconolactone (green, protein and lactone; magenta, zinc; and red, water) and $NADP^+$/Zn/glucose structures (orange; zinc large sphere, water small sphere), showing the movement of the zinc and its associated water between the 2 complexes, and (*E*) an overlap of the structures of the GlcDH lactone complex, (green magenta, zinc), *T. brockii* ADH (purple, 1ykf, ref. 38), human SDH (blue, 1pl6, ref. 11), and LADH (light brown, 1heu, ref. 17).

involving the nucleotide cofactors. These structures have provided a largely static view of the active site in the MDR superfamily, and the implications for the mechanism of any differences that are observed is hampered by the fact that the structures relate to the study of mutants, or inhibitor complexes, whose relationship to the reaction intermediates is unclear. This situation is also compounded by difficulties associated with the comparison of what are essentially different, although related enzymes. The question that arises from the work presented here is whether the dynamic changes in the active site seen in glucose dehydrogenase have any relevance to the wider superfamily.

Clearly, the EXAFS (10) and EPR (8) studies on MDR family members support the idea of dynamic changes during catalysis. At the structural level a global comparison of the active sites of different members of this superfamily reveal them to be closely related to each other and to GlcDH, strongly suggesting that at least some of the features seen here may be of wider significance (Fig. 1*E*). Of the four residues in GlcDH that coordinate the Zn at different stages of catalysis, two (His-63 and Glu-64) are strictly conserved across the family (equivalent to His-67 and Glu-68 in LADH). The other two residues involved in zinc coordination (Asp-38 and Glu-150 in GlcDH) are invariably either acidic or cysteine residues within the family. In addition, two further strongly conserved residues are found close to the zinc centre: Gly-62, which is involved in the correct positioning of His-63, and Asp-41, which lies adjacent to the side chain of His-63 (equivalent to Gly-66 and Asp-49 in LADH, respectively).

The dramatic movements of the zinc and water in the active site of the GlcDH complexes have not yet been mirrored in crystallographic studies of any other MDR family member. One reason for this may simply be because of the limitation of the range of complexes whose structures have been determined on other enzymes in the family. However, some indications that movements might occur in other MDR enzymes have been reported from analyses of crystal structures. For example, a comparison of the binary SDH/NAD^+/Zn^{2+} complex with that of SDH in complex with NAD^+, Zn^{2+}, and an inhibitor shows a rearrangement of the zinc ligands accomplished, in part, by the movement of the zinc away from the side chain of Glu-70 (equivalent to Glu-64 in GlcDH), and toward the inhibitor, by 2.3 Å (11). A similar movement of the zinc away from the conserved glutamate residue and toward the substrate is seen between the binary and ternary complexes of glutathione-dependent formaldehyde dehydrogenase (23). However, in this ternary complex structure the zinc movements are accompanied by a small reorientation of the protein ligands and no zinc-bound water molecule has been identified, although the limited resolution of the analysis would make such identification difficult. In addition, an atomic resolution structure of LADH with NADH (17) shows alternative conformers for Glu-68 (Glu-64 in GlcDH), one of which adopts the orientation seen in GlcDH and forms a ligand to the zinc, whereas the other does not.

Implications for Active-Site Dynamics in Catalysis by the MDR Superfamily. The classical mechanism of the MDR family requires that the zinc bound water in the binary complex be displaced by the substrate (2). However, in both ternary complexes of GlcDH, the zinc-bound water is retained, a situation also observed in the structures of an inactive T40A mutant of *S. solfataricus* glucose dehydrogenase, in complex with either glucose and xylose (24) and also in an inhibitor complex of sorbitol dehydrogenase (11). These structures therefore dispel the view that the substrate displaces the water as a universal feature of the mechanism of the MDR family.

The dynamic behavior shown by the zinc and its bound water in GlcDH is also not consistent with the classical view of catalysis by the MDR family. Rather, it supports the alternative reaction mechanism that has been proposed and involves the formation of a number of penta-coordinate zinc intermediates (6, 7, 24). Although the zinc is tetrahedrally coordinated in each of the GlcDH complexes, six different zinc ligands are used in total. The movement of the zinc ion and the water molecule during the

Table 1. Distances in Å between the Zn and selected residues in the binary and ternary complexes of GlcDH

	Distance to Zn ion in each GlcDH complex structure			
Complex	$NADP^+$/Zn	$NADP^+$/Zn/glucose	$NADP^+$/Zn/lactone	NADPH/Zn
Asp 38 OD2*	2.87	**2.02**	**2.09**	4.19
His 63 NE2	**2.15**	**1.98**	**2.14**	**2.32**
Glu 64 OE2	**2.30**	3.65	**2.14**	**2.28**
Glu 150 OE1	**2.35**	3.73	3.35	**2.18**
W1	**1.71**	**1.94**	**1.83**	**2.18**
Substrate O1	n/a	**2.01**	3.60	n/a

The distances for the 4 ligands made to the Zn in each complex are highlighted in bold. n/a, not applicable.
*For the NADPH/Zn complex the OD1 atom of D38 is closest to the Zn, as a different rotamer is present in this structure.

reaction, seen in the study presented here, suggests that at least three different transient five-coordinated zinc species are formed. The first would be associated with the conversion of the binary complex with $NADP^+$ to the ternary complex with glucose, the second could be formed as the glucose is oxidized to the lactone, and the third as the lactone leaves the active site. Consistent with the proposed formation of such transient five-coordinated species by XAFS studies on alcohol dehydrogenase from *T. brockii* (10), the X-ray structures perhaps suggest that dynamic changes in the active site are a common feature in the MDR family.

Biochemical, biophysical, and computational studies have suggested that as zinc is a strong Lewis acid, the water molecule it coordinates would be an hydroxide ion in the binary complex, as proposed for LADH (25), SDH (11, 26), and *S. solfataricus* GlcDH (24). This hydroxide could then act as a base to transiently trap the proton released during formation of the alkoxide. However, the protonation state of this water could vary as it and the zinc move in response to the formation of the different complexes. In particular, the movement of the water from its relatively exposed position in the binary complex with nucleotide to its position between the zinc and the two carboxyl groups of Glu-64 and Glu-150 in the ternary complex with glucose, would be anticipated to raise its pK_a considerably, favoring the shuttling of the proton from the glucose to the hydroxide as the alkoxide is formed. Subsequently, movement of the positively charged zinc ion away from the substrate O1 and toward the position it adopts in the lactone complex would destabilize the alkoxide; promoting its collapse, the concomitant hydride transfer of the substrate C1 hydrogen to the nicotinamide ring of the coenzyme and release of the proton to the bulk solvent, thus completing the reaction. In this mechanism, the need for a proton-relay system to the solvent (2) has been removed and is replaced by a simpler solution to the fate of the proton abstracted from the alcohol at the start of catalysis.

A further consequence of the movement of the zinc away from Glu-64 and Glu-150 and toward Asp-38 as the alcohol approaches to coordinate the zinc, is the replacement of these two carboxyl groups as zinc ligands by the single carboxyl of Asp-38 and the substrate hydroxyl. This reduction in net charge on the ligands remains until the last step of the reaction, despite subsequent ligand exchanges (Fig. 2). These differences would transiently raise the positive charge on the zinc during the reaction, consistent with the observed increase in positive charge on the zinc seen in single turnover kintetic XAS studies on the alcohol dehydrogenase from *T. brockii* (10). This correlation further suggests that the zinc and water movements seen in GlcDH may well occur in other members of the MDR family.

Given the similarity in active site architecture in the MDR superfamily, it would seem unlikely that these enzymes would operate by distinctly different mechanisms and a proposal that unifies the body of data that has accumulated so far would appear to be required. The movement of the zinc and its use of different ligands during the catalytic cycle seen in this set of GlcDH complex structures is not dissimilar to that observed in formaldehyde dehydrogenase (23) and provides such a unifying view, suggesting that in these enzymes the catalytic mechanism has more facets than has been previously thought.

In the discussion above we do not suggest that the work presented here provides a definite answer to the mechanism of the MDR superfamily. However, the fact that the movements of the zinc and the water, together with the associated electronic changes on the zinc described here for the GlcDH substrate complexes agree closely with the studies on *T. brockii* ADH, and together with the similarities seen for formate dehydrogenase, does suggest that the textbook MDR mechanism requires modification. This work also provides a structural framework around which the catalytic events of this enzyme family can be investigated and which may provide a more complete description of the roles of the various functional groups than has hitherto been possible. Indeed, such changes in zinc coordination during the catalytic cycle have also been observed in other metalloenzymes, such as the matrix metlloproteinases (27, 28) and TNF-α converting enzyme (29), perhaps suggesting that active site dynamic coordination chemistry is an ubiquitous process in zinc metalloenzymes.

Methods

Crystals of *Haloferax mediterranei* glucose dehydrogenase were grown as described previously (30, 31), in the presence of zinc (1 mM) and either 5 mM

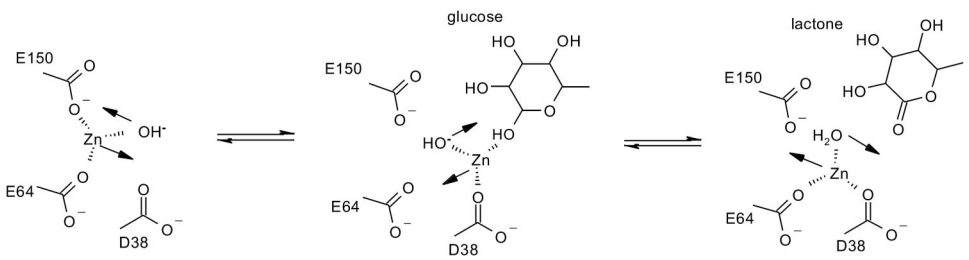

Fig. 2. A schematic diagram, viewed down the His 63 Ne2–Zn bond, of the zinc ligands in the NADP(H)/Zn complex (*Left*), $NADP^+$/Zn/glucose complex (*Center*), and $NADP^+$/Zn/gluconolactone complex (*Right*). The arrows give the direction of the movement of the zinc and water between the complexes.

Table 2. Data collection and refinement statistics

Data set	NADPH/Zn	$NADP^+$/Zn	$NADP^+$/Zn/glucose	$NADP^+$/Zn/gluconolactone
PDB code	2vwp, r2vwpsf	2vwq, r2vwqsf	2vwh, r2vwhsf	2vwg, r2vwg
Space group	I222	I222	I222	I222
Unit cell parameters, Å				
a	60.6	61.9	61.5	61.6
b	107.7	111.1	112.7	112.2
c	153.6	152.2	151.5	150.6
Temperature, K	100	290	290	290
Resolution, Å	2.01	2.1	2.03	2.0
High res shell, Å	2.01–2.08	2.10–2.15	2.03–2.08	2.0–2.05
R_{merge}, %*,†	0.059(0.35)	0.066(0.39)	0.081(0.28)	0.049(0.36)
Completeness, %†	94.5 (82.5)	90.0(91.6)	98.9(89.9)	98.9(99.2)
Multiplicity	3.9 (3.4)	3.0(2.1)	6.8(2.3)	7.7(2.6)
$I/\sigma I$ †	30.1 (3.7)	22.7(2.5)	18.27(3.7)	17.39(2.9)
Refinement				
No. of reflections used	30211	28810	32244	33477
R_{cryst} (%) /R_{free} (%)	18.4/22.2	14.3/17.5	13.4/15.9	13.5/15/9
Ramachandran favoured/outliers, %‡	96.3/0	97.2/0.28	97.5/0	97.2/0
Rms deviation bond length, Å	0.012	0.011	0.009	0.009
Rms deviation bond angle, deg	1.29	1.277	1.224	1.222
No. in final model				
Residues	357	357	357	357
Protein atoms	2770	2770	2770	2770
Catalytic Zn^{2+}	1	1	1	1
NADP	1	1	1	1
Water molecules	245	116	148	143
Mean B-values, $Å^2$				
Protein atoms	30.6	37.6	35.6	41.4
NADP(H)	37.5	32.7	28.7	33.7
Substrate	–	–	26.9	32.9
Catalytic Zn^{2+}	34.7	44.6	27.9	43.9
Waters	35.7	42.0	42.7	47.4

*$R_{merge} = \Sigma_{hkl}\ I_i - I_m\ /\Sigma_{hkl}\ I_m$, where I_m is the mean intensity of the reflection.
†Numbers in parentheses indicate values for the highest resolution shell.
‡Molprobity analysis (39).

$NADP^+$, by using sodium citrate as the precipitant (1.4–1.6 M sodium citrate, 100 mM Hepes, pH 7.0, and 2 M NaCl) or 5 mM NADPH, using 2-methyl-2,4-pentanediol (MPD) as precipitant (67–72% MPD, 100 mM Hepes, pH 7.5, and 2 M NaCl). To obtain the ternary complexes, single crystals grown in the presence of $NADP^+$ and zinc were soaked in a solution of mother liquor containing 10 mM D-glucose or β-D-1,5 gluconolactone for 1 h, respectively.

Data were collected by using the rotation method, on a MarResearch image plate using CuKα X-rays generated by either a Rigaku RU200 rotating anode generator with Yale Mirrors or a Rigaku MM007 generator with Osmic Varimax optics. Data for the crystals grown in the presence of sodium citrate were collected at 293 K, whereas for the crystals grown in the presence of MPD the crystals were flash cooled straight from the drop and data collected at 100 K. The data were initially processed by using Denzo/Scalepack (32) and subsequently analyzed with the CCP4 suite (33) (Table 2). All of the crystals belong to space group I222, with approximate cell dimensions a = 61.5 Å, b = 112.7 Å, and c = 151.5 Å (Table 2), and with a monomer in the asymmetric unit. For each structure, phases were determined by molecular replacement by using the program Amore (34) and the coordinates of the metal free enzyme as the search model [pdb code 2B5V (21)]. Initial electron density maps for each structure, produced with Refmac5 (35) contained clear features for the zinc and cofactor. In addition, the maps for the two ternary complexes had unambiguous density features corresponding to either ß-D glucose or D-glucono-1,5 lactone, respectively. Iterative cycles of refinement and rebuilding [using Coot (36)] with water molecules added during the process, yielded final models for each of the structures (Table 2). In all of the structures the electron density was generally of good quality, with only residues 7–12, which connect the first two beta strands, poorly defined. In addition, the loop formed by residues 46–49 had weak density in the $NADP^+/Zn^{2+}$ structure, but this loop was clear for the other three structures. Color figures prepared by using PyMOL.

To remove small negative density peaks at the zinc site in the sigmaA-weighted (37) mF_o–DF_c difference maps for the two ternary complexes, the occupancy of the zinc was set to 0.8. The position of the zinc and zinc-bound water atoms in each complex were checked by calculating omit maps, with these two atoms missing. Inspection of the resulting difference maps confirmed the location of the zinc and its bound water (Fig. S2). Additionally, in the GlcDH/$NADP^+$/Zn/glucose complex, a small, positive, electron-density peak, corresponding in position to that of the zinc in the lactone complex, could be seen, perhaps suggesting that there had been some limited turnover of the glucose to lactone within in the crystal during the time course of the experiment. However, as no alternate positions could be seen for the glucose C1 and O1 atoms, or the zinc bound water molecule, the proportion of species other than the glucose must be small.

ACKNOWLEDGMENTS. We thank Professor Bob Williams for helpful discussions on the manuscript. This work was supported by the Biotechnology and Biological Sciences Research Council, the Wellcome Trust, The Woolfson Foundation, and Spanish Ministry of Science and Education and by Program for Formation of Researchers (FPI) fellowships from Generalitat Valenciana (Spain) to J.E.

1. Auld DS (2001) Zinc coordination sphere in biochemical zinc sites. *Biometals* 14:271–313.
2. Eklund H, Plapp BV, Samama JP, Branden CI (1982) Binding of substrate in a ternary complex of horse liver alcohol dehydrogenase. *J Biol Chem* 257:14349–14358.
3. Eklund H, Brändén C-I (1987) Alcohol dehydrogenase. In *Biological Macromolecules and Assemblies* (Wiley, New York) pp 73–143.
4. Eklund H, Horjales E, Jornvall H, Branden CI, Jeffery J (1985) Molecular aspects of functional differences between alcohol and sorbitol dehydrogenases. *Biochemistry* 24:8005–8012.
5. Pettersson G (1987) Liver alcohol dehydrogenase. *CRC Crit Rev Biochem* 21:349–389.
6. Dworschack RT, Plapp BV (1977) pH, isotope, and substituent effects on the interconversion of aromatic substrates catalyzed by hydroxybutyrimidylated liver alcohol dehydrogenase. *Biochemistry* 16:2716–2725.
7. Makinen MW, Maret W, Yim MB (1983) Neutral metal-bound water is the base catalyst in liver alcohol dehydrogenase. *Proc Natl Acad Sci USA* 80:2584–2588.

8. Makinen MW, Yim MB (1981) Coordination environment of the active-site metal ion of liver alcohol dehydrogenase. *Proc Natl Acad Sci USA* 78:6221–6225.
9. Sytkowski AJ, Vallee BL (1978) Cobalt exchange in horse liver alcohol dehydrogenase. *Biochemistry* 17:2850–2857.
10. Kleifeld O, Frenkel A, Martin JM, Sagi I (2003) Active site electronic structure and dynamics during metalloenzyme catalysis. *Nat Struct Biol* 10:98–103.
11. Pauly TA, *et al.* (2003) X-ray crystallographic and kinetic studies of human sorbitol dehydrogenase. *Structure* 11:1071–1085.
12. Al-Karadaghi S, Cedergren-Zeppezauer ES, Hovmoller S (1994) Refined crystal structure of liver alcohol dehydrogenase-NADH complex at 1.8 Å resolution. *Acta Crystallogr D Biol Crystallogr* 50:793–807.
13. Ganzhorn AJ, Plapp BV (1988) Carboxyl groups near the active site zinc contribute to catalysis in yeast alcohol dehydrogenase. *J Biol Chem* 263:5446–5454.
14. Bauer R, *et al.* (1991) Coordination geometry for cadmium in the catalytic zinc site of horse liver alcohol dehydrogenase: Sudies by PAC spectroscopy. *Eur Biophys J* 20:215–221.
15. Formicka G, Zeppezauer M, Fey F, Huttermann J (1992) Copper(II)-substituted horse liver alcohol dehydrogenase: Sructure of the minor species. *FEBS Lett* 309:92–96.
16. Ryde U (1995) On the role of Glu-68 in alcohol dehydrogenase. *Protein Sci* 4:1124–1132.
17. Meijers R, *et al.* (2001) On the enzymatic activation of NADH. *J Biol Chem* 276:9316–9321.
18. Pire C, Camacho ML, Ferrer J, Hough DW, Bonete MJ (2000) NAD(P)$^+$-glucose dehydrogenase from *Haloferax mediterranei*: Kinetic mechanism and metal content. *J Mol Catal B: Enzym* 10:409–417.
19. Bonete MJ, Pire C, Fi LL, Camacho ML (1996) Glucose dehydrogenase from the halophilic Archaeon Haloferax mediterranei: Enzyme purification, characterisation and N-terminal sequence. *FEBS Lett* 383:227–229.
20. Pire C, Esclapez J, Ferrer J, Bonete MJ (2001) Heterologous overexpression of glucose dehydrogenase from the halophilic archaeon Haloferax mediterranei, an enzyme of the medium chain dehydrogenase/reductase family. *FEMS Microbiol Lett* 200:221–227.
21. Britton KL, *et al.* (2006) Analysis of protein solvent interactions in glucose dehydrogenase from the extreme halophile Haloferax mediterranei. *Proc Natl Acad Sci USA* 103:4846–4851.
22. Rossmann MG, Moras D, Olsen KW (1974) Chemical and biological evolution of nucleotide-binding protein. *Nature* 250:194–199.
23. Sanghani PC, Bosron WF, Hurley TD (2002) Human glutathione-dependent formaldehyde dehydrogenase. Structural changes associated with ternary complex formation. *Biochemistry* 41:15189–15194.
24. Milburn CC, *et al.* (2006) The structural basis of substrate promiscuity in glucose dehydrogenase from the hyperthermophilic archaeon Sulfolobus solfataricus. *J Biol Chem* 281:14796–14804.
25. Meijers R, *et al.* (2007) Structural evidence for a ligand coordination switch in liver alcohol dehydrogenase. *Biochemistry* 46:5446–5454.
26. Klimacek M, Hellmer H, Nidetzky B (2007) Catalytic mechanism of Zn2+-dependent polyol dehydrogenases: Kinetic comparison of sheep liver sorbitol dehydrogenase with wild-type and Glu154→Cys forms of yeast xylitol dehydrogenase. *Biochem J* 404:421–429.
27. Bertini I, *et al.* (2006) Snapshots of the reaction mechanism of matrix metalloproteinases. *Angew Chem Int Ed Engl* 45:7952–7955.
28. Rosenblum G, *et al.* (2007) Molecular structures and dynamics of the stepwise activation mechanism of a matrix metalloproteinase zymogen: Challenging the cysteine switch dogma. *J Am Chem Soc* 129:13566–13574.
29. Solomon A, Akabayov B, Frenkel A, Milla ME, Sagi I (2007) Key feature of the catalytic cycle of TNF-alpha converting enzyme involves communication between distal protein sites and the enzyme catalytic core. *Proc Natl Acad Sci USA* 104:4931–4936.
30. Esclapez J, *et al.* (2005) Crystallization and preliminary X-ray analysis of binary and ternary complexes of Haloferax mediterranei glucose dehydrogenase. *Acta Crystallogr F* 61:743–746.
31. Ferrer J, *et al.* (2001) Crystallization and preliminary X-ray analysis of glucose dehydrogenase from Haloferax mediterranei. *Acta Crystallogr D* 57:1887–1889.
32. Otwinowski Z, Minor W (1997) Processing of X-ray diffraction data collected in oscillation mode. *Macromolecular Crystallography*, *Pt A* 276:307–326.
33. Collaborative Computational Project, Number 4 (1994) The CCP4 suite: Programs for protein crystallography. *Acta Crystallogr D* 50:760–763.
34. Navaza J (2001) Implementation of molecular replacement in AMoRe. *Acta Crystallogr D* 57:1367–1372.
35. Murshudov GN, Vagin AA, Dodson EJ (1997) Refinement of macromolecular structures by the maximum-likelihood method. *Acta Crystallogr D* 53:240–255.
36. Emsley P, Cowtan K (2004) Coot: Model-building tools for molecular graphics. *Acta Crystallogr D* 60:2126–2132.
37. Read RJ (1986) Improved Fourier coefficients for maps using phases from partial structures with errors. *Acta Crystallogr A* 42:140–149.
38. Korkhin Y, *et al.* (1998) NADP-dependent bacterial alcohol dehydrogenases: Crystal structure, cofactor-binding, and cofactor specificity of the ADHs of Clostridium beijerinckii and Thermoanaerobacter brockii. *J Mol Biol* 278:967–981.
39. Davis IW, *et al.* (2007) MolProbity: All-atom contacts and structure validation for proteins and nucleic acids. *Nucleic Acids Res* 35:W375–383.